Design Experiences of the First Solar Parabolic Thermal Power Plant for Various Regions in Iran

K. Azizian, M. Yaghoubi , A. Kenary
Solar Thermal Power Project, Engineering School, Shiraz University

ABSTRACT:
The basic design is made for a 250 kw solar power plant. The main element of the plant is the collectors. Base on system simulation, a parabolic collector constructed and tested for one year. The model is first validated with experimental measurement and a detail numerical model is also developed to study effects of various optical properties of mirrors and receiver on the thermal performance of the collectors. It is observed that due to poor optical properties of the present collector, it would not be able to produce hot oil with desired temperature. Improving the material of the mirrors and the receiver tube, thermal performances exceed substantially from the design conditions. By considering available optical properties simulation is made to estimate yearly steady and unsteady behavior and the performance of the power plant for three locations: Shiraz, Yazd and Lar in Iran. Comparison of the yearly performance of the cycle shows that unsteady behavior reveals different results and simulations approach a reliable technique to study such cycle.

Keywords: Solar thermal, parabolic trough, optical simulation, performance, optical properties.

[Downloaded from necjournals.ir on 2026-11-18]

Introduction

Sustainable energy is energy that, in its production or consumption, has minimal negative impacts on human health and the healthy functioning of vital ecological systems, including the global environment. It is an accepted fact that solar energy is a sustainable form of energy, which has attracted more attentions during the recent years [1].

There are numerous techniques for the effective concentration of the sun's energy to electricity generation. One of these techniques is compound parabolic concentrator [2]. Iran with great amount of land is located on the belt of the world sun and it is one of the countries, which has substantial amount of good solar irradiance. In most part of Iran and specially in the south-central part, where the city of Shiraz in located, there is at least 300 sunny days in a year and average yearly clearness index is greater than 0.67 [3].

Great amount of renewable energy potential, environmental impact as well as economic consideration of fossil fuel consumption and high emphasis of sustainable development for the future, are the main consideration that led the Deputy Ministry of Energy of Iran to define, support and install the first 250 kW pilot solar thermal power plant (as shown in Fig 1) in Shiraz, Iran. The plant is designed to generate 250 kW of electricity continuously to be feed to the national grid. To achieve this goal a hybride-Rankine system contains two cycles of hot oil and steam in selected. The plant consists of:

i) A field of 8 parallel loops of 6 solar parabolic trough collectors.
ii) A Rankine steam cycle.
iii) An oil cycle.
iv) A heat storage system.

The collectors are parabolic trough 25 m length, 3.4 m wide with 0.88 m focal length [4]. More details of collectors are in Table 1.

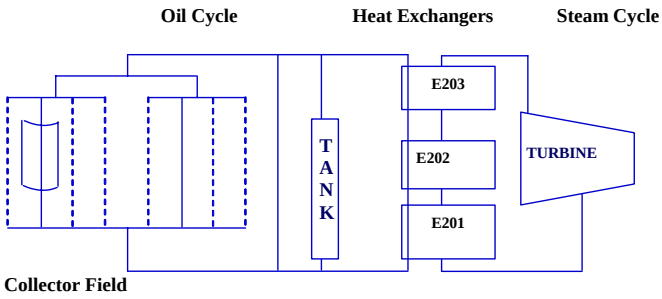


Fig.1- Flow Schematic of Power Plant

[Downloaded from necjournals.ir on 2026-11-18]

Table 1- Collector parameters

Width	3.4 m	Rim angle	90 ^{o}
Length	25 m	Reflectivity of mirror	0.47
Aperture	3.1 m	Transmissivity of cover	0.82
Focal length	88 cm	Emissivity of cover	0.88
Outer diameter of receiver	4.2 cm	Absorptivity of receiver	0.74
Inner diameter of receiver	3.5 cm	Emissivity of receiver	0.45
Outer diameter of cover	7 cm	Intercept factor	0.7
Inner diameter of cover	6.7 cm	Mass flow rate	1 kg/s
Concentration ratio	26	$\rho\tau\alpha$	0.285

Prior to construct the plants, a sample of the collector is built and tested for more than 12 months. Collector is installed in the north-south direction and rotates from east-to-west with special hydraulic pump and jacks system an illustrated in Fig. 2. The collector system, Fig. 3, contains a computer automatic sun tracking sensor, a wind velocity measuring sensor, an orifice flow meter, a Kipp&Zonen Pyroheliometer to measure direct solar irradiance, a computer data acquisition system, a storage tank and a hot oil circulating pump.



Fig.2-Typical view of the collector installed north-south direction

[Downloaded from necjournals.ir on 2026-11-18]

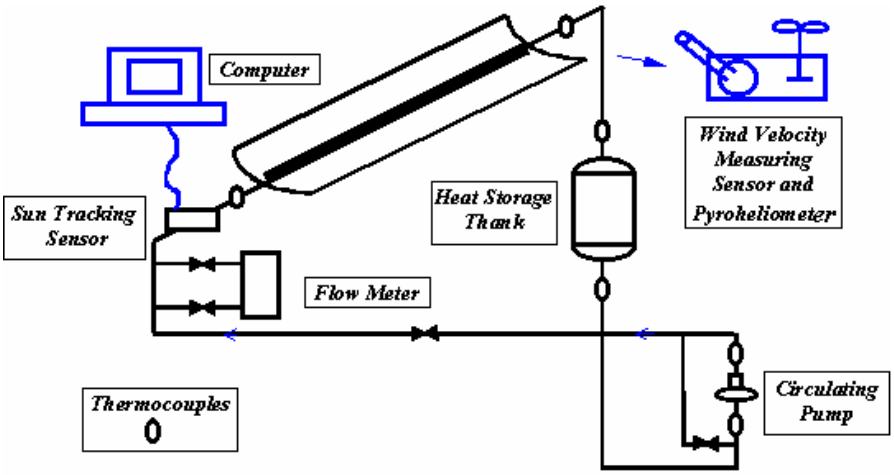


Fig. 3- Flow schematic for experimental apparatus of the parabolic trough collector

The objective of the present article is to simulate numerically the above collector system and to study its transient thermal performances for several days of operation and compare the numerical results with field experimental measurements. Attempt is also made to change the design variable to enhance thermal efficiency of the collector.

From the design consideration, a thermal performance of a collector is mainly related to the optical properties of the receiver, and mirrors. To change optical properties such as, mirror reflectivity, glass transmissivity, receiver tube absorptivity and emissivity, the program is able to simulate the system and illustrate the effects on the effectiveness of the collector and finally on the over all performances of the field of 48 collectors. Several selections are made to optimize the collector effectiveness and results are implemented on the thermal performances of solar collectors' field and the overall power plant efficiency of the system under consideration. By considering more realistic optical properties simulation is carried out and results for Shiraz, Yazd and Lar are presented.

Collector Experimental Measurements

The collector system, shown in Fig. 3, operating from sunrise to sunset. Measurements are made every 30 min intervals, from the following parameters.

1- Oil inlet and outlet temperature from the receiver
2- Oil mass flow rate
3- Wind velocity and ambient temperature

[Downloaded from necjournals.ir on 2026-11-18]

4- Solar irradiance
5- Glass tube temperature.

Measurements conducted only for the sunny days and the data are stored in a computer for the entire day.

Collector Cycle Simulation

Oil circulates through a pump and temperature sensors of type PT100, measure inlet and outlet temperatures of the oil in the receiver tube. In order to make a transient simulation of the mirror, receiver and circulating oil, an element of dx along the tube is selected as show in Fig. 4.

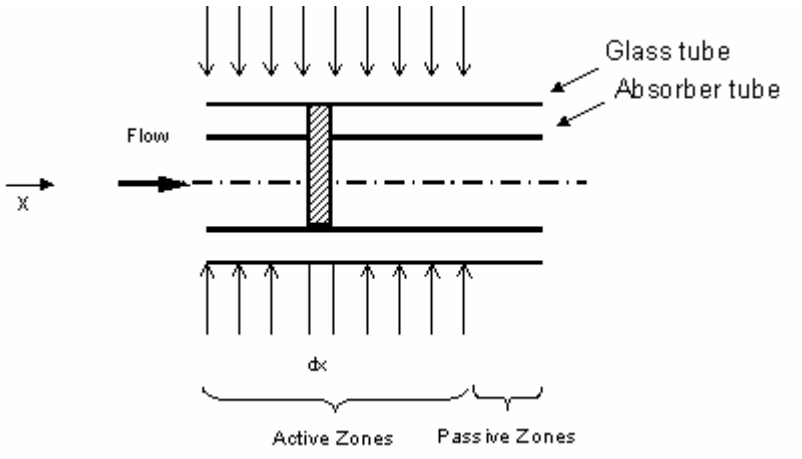


Fig. 4- A section of the receiver tube

By applying the instantaneous energy balance between hot oil, tube wall, and glass cover, the following equations can be derived [5-7].

Hot Oil:

$$(1)\quad \rho_f C_f A_f\left(\frac{\partial T_f}{\partial t}+V\frac{\partial T_f}{\partial x}\right)=U_C\pi d_{r_i}\left(T_m-T_f\right)$$

Tube wall:

$$(2)\quad \rho_m C_m A_m\left(\frac{\partial T_m}{\partial t}\right)=\eta_o G I_b - U_L\pi d_{r_o}\left(T_m-T_a\right)-U_C\pi d_{r_i}\left(T_m-T_f\right)$$

[Downloaded from necjournals.ir on 2026-11-18]

Glass cover:

$$(3)\quad \rho_c C_c A_c\left(\frac{\partial T_c}{\partial t}\right) = \frac{\eta_o}{\tau\alpha} G I_b \alpha_c - H_{c-a}\pi d_{c_o}\left(T_c - T_a\right) - H_{c-r}\pi d_{c_i}\left(T_c - T_m\right)$$

The glass tube effect is included to increase accuracy of energy exchange from the receiver.

All the parameters are defined in the nomenclature. Direct solar irradiation can be measured by a Pyroheliometer or can be determined by the relation given by Daneshyar [8] for Iran cities as follows:

$$(4)\quad I_b = I_0 \times \left(1 - C_{fa}\right)\left\{1 - \exp\left[-0.075\left(\frac{\pi}{2} - \theta_z\right)\right]\right\}$$

For Shiraz, I_0=960 W/m^2 and cloud factor C_f is taken 0.097 during September.

To write these equations, following assumptions made:

a) Heat loss from the absorber tube is by convection and radiation.

b) Physical properties of air and oil are function of temperature and;

Oil properties are:

$$(5)\quad k_f = 0.1882 - 8.304\times10^{-5}\times\left(T_f + 273.15\right),\ \text{W/m}\,^{o}\text{C}$$

$$(6)\quad C_f = 0.8132 + 3.706\times10^{-3}\times\left(T_f + 273.15\right),\ \text{kJ/kg}\,^{o}\text{C}$$

$$(7)\quad \rho_f = 1071.76 - 0.72\times\left(T_f + 273.15\right),\ \text{kg/m}^3$$

c) Flow is uniform at any section of the tube.

d) Solar irradiance is time depend.

e) Axial heat conduction in the glass tube and absorber is negligible.

f) The value of optical efficiency can be found as [9]

$$(8)\quad \eta_o = \left[K(\theta)\right]\left[\rho\left(\tau\alpha\right)_n\right]\gamma$$

Values of mirror reflectivity ρ, glass cover transmissivity τ, and the receiver absorptivity α, are measured experimentally as cited by Ref. [4, 10] and shown in table 1.

The intercept factor γ, which is defined as the fraction of those rays incident on the aperture that are intercepted by the receiver depends on optical errors, sun shape, rim angle and concentration ratio [11]. Incidence-angle modifier $K(\theta)$ in Eq (8) is measured according to ASTM code [12] and its variation with respect to time is around 0.3 [10]. For normal operation this value should be around one, but the present measurements indicate that it is much less than one. This may be

[Downloaded from necjournals.ir on 2026-11-18]

due to un-appropriate material of mirror glass and surface coating of it, as well as the mirror non-alignments. The corresponding value of K(θ) for the mirror fabricated by LUZ industries during the day is about one [10]. Strong variation of the modified incident angle will affect the over all thermal performances of the collector and the power plant efficiency.

For storage tank, stratification and buoyancy effect is considered and the corresponding differential equation for the oil temperature in the tank resulted from energy balance is

$$\frac{\partial T_f}{\partial t} = \frac{k_f}{\rho_f C_f}\frac{\partial^2 T_f}{\partial x^2} - \frac{\dot{m}_f}{\rho_f A_f}\frac{\partial T_f}{\partial x} + \frac{UP}{\rho A_f C_f}\left(T_f - T_a\right) \quad (9)$$

The oil temperature during charging is given as $T(0,t)= T_{ch}$ and for discharging is $T(1,t)= T_{dc}$.

Transient heat losses from the oil in the pipes is also considered, and from thermal balance for a section of the pipe with length dx is

$$\dot{m}_f C_f \frac{\partial T_f}{\partial x} = U\ P_p\left(T_f - T_a\right) + \rho_f A_f C_f \frac{\partial T_f}{\partial t} \quad (10)$$

Inlet oil temperature to each section is assumed equal to the outlet temperature of the downstream section**.**

Results

In this section initially results of measurement collector performance will be given, then its performance for the optical properties will be presented. Based on accepted optical specifications power plant cycle simulation is continued.

The system of ordinary differential Eqs. (1,2,3,10) is solved numerically by finite difference method implying implicit scheme and Eq.(9) is solved numerically by finite difference implying explicit scheme. The iteration start from a uniform temperature for the system equal to ambient temperature and converged solution is obtained for each five min intervals. To run the program for the collector with specification presented in Table 1, several inputs such as variation of ambient temperature, oil flow rate, wind velocity and solar irradiation are given. Solar irradiation is also available by specific correlation for the region. Typical measurements as well as numerical computation of temperature variation during a day are illustrated in Fig.5. For this graph oil mass flow rate is 1 kg/s and experimental data correspond to 17th Sep. 2000, where wind velocity was about 7 m/s. The maximum difference between measured and calculates values of temperature is 6%. Oil inlet and outlet

[Downloaded from necjournals.ir on 2026-11-18]

temperature rise continuously with a small differences up to 3 PM and then they start to decrease in the afternoon. Maximum temperature of the oil is about 142 °C while for glass tube it is around 78 °C, which is due to high absorptivity of the glass tube. Although solar radiation are considerable but the temperature rise is far from design point. This is mainly due to poor optical properties of the mirrors as well as the glass tube. In Fig.6 measured solar irradiation, optical efficiency and thermal efficiency of the collector is plotted for the same day. It shows that although the sky is clear, but the efficiencies are not satisfactory, which is due to poor optical materials.

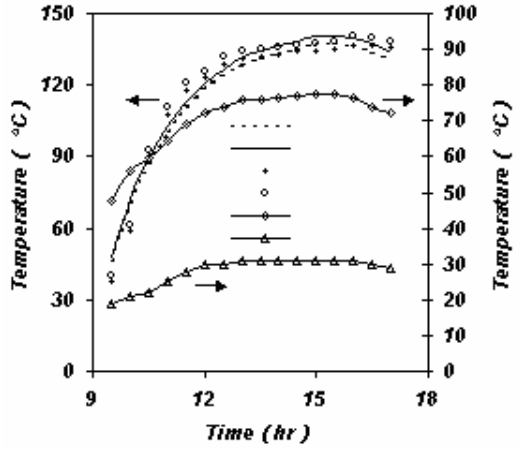


Fig. 5- Comparison of measured and computed temperature in receiver

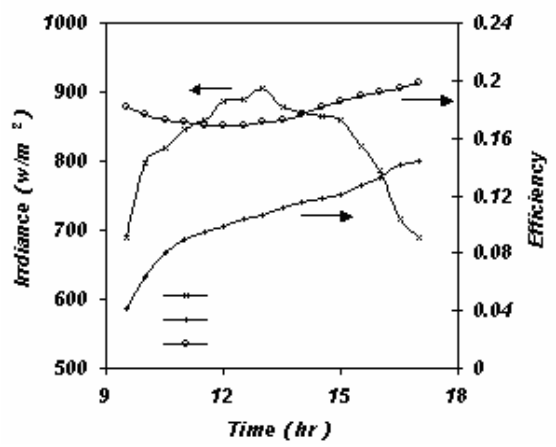


Fig. 6-Measurments of solar irradiation and efficiency of the collector during a day

[Downloaded from necjournals.ir on 2026-11-18]

In Fig.7 temperature rise of the oil in the receiver is calculate by simulation using measured sunshine irradiation, and also employing Daneshyar's correlation [8]. It shows that Daneshyar correlation produces only very negligible error relative to the measurements and hence it is relatively accurate to simulate the collector system by relation (4). This figure also shows that there are some variations in the measured values of temperature rise near the noon. This is mainly due to tracking errors, which increases near the noontime.

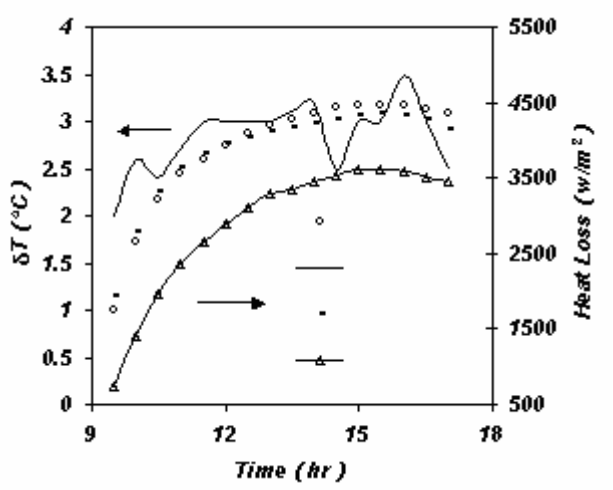


Fig. 7- Oil temperature difference between outlet and inlet of the receiver (D=Daneshyar model, E=experimental, N=numerical method)

To study effects of optical properties of the collector on the thermal performances of the collector, simulation is carried out for the same day for various reflectivity of mirror ρ, transmissivity of cover τ , absorptivity of receiver α, intercept factor γ and results of the temperature rise of the oil in the receiver is determined as illustrated in Figs. 8-12. In these figures all the optical properties are taken constant, except one property. Figure 8 shows effects of receiver absorptivity on the temperature rise of the oil in the receiver. It shows that the effect is relatively considerable although the value α varied from 0.55 to 0.95. Similar results are obtained by changing emissivity of the tube from 0.55 to 0.1 in Fig.9. It shows that the effect is much less on the temperature rise.
Figure 10 illustrate effects of various intercept factor on the oil temperature rise. The value γ in this figure is changed from 0.65 to 0.95. Fig. 10 illustrate that the performance increases by increasing γ. For 0.1 increment of γ, temperature rise is about 0.25 °C, which is about 20 percent.

[Downloaded from necjournals.ir on 2026-11-18]

Effects of reflectivity of mirror on the temperature rise of oil in the receiver are more pronounced. Figure 11 illustrates such effect for reflectivities of 0.35 to 0.95. Poor mirrors reduced considerately temperature rise and hence thermal efficiency of collector. It should be noted that in this figure, the other optical properties of collector are taken equivalent to the present collector. Poor performance of the collector as shown in Fig. 5 is partially from lower mirrors reflectivity. Figure 12 presents effects of glass tube transmissivity on the temperature rise of the oil in the receiver. For the present collector, the glass has $\tau \approx 0.8$ and it reduces the performance about 10%.

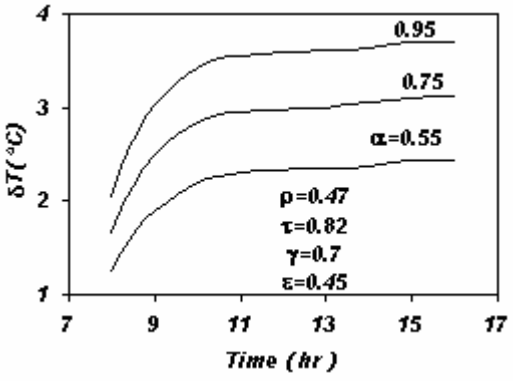


Fig.8- Effects of various tube absorptivity on oil temperature rise in the receiver

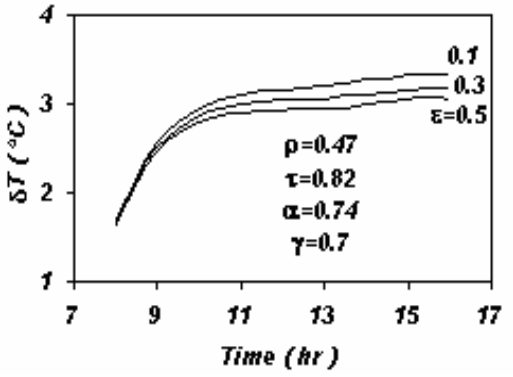


Fig. 9-Effects of tube emissivity on the oil temperature

[Downloaded from necjournals.ir on 2026-11-18]

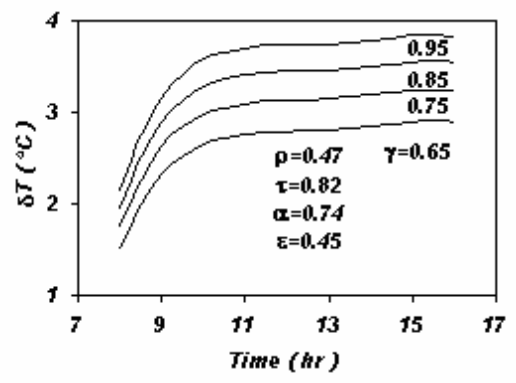


Fig. 10-Effects of various intercept factor on the oil temperature rise in the receiver

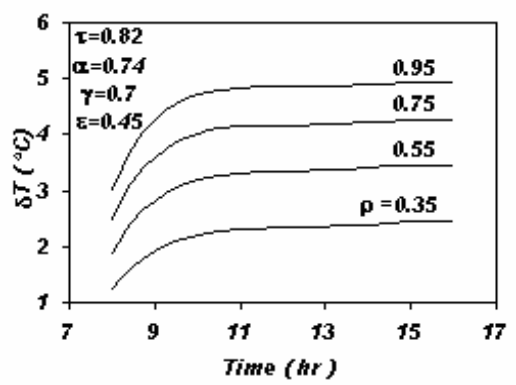


Fig. 11-Effects of mirror reflectivity on the oil temperature

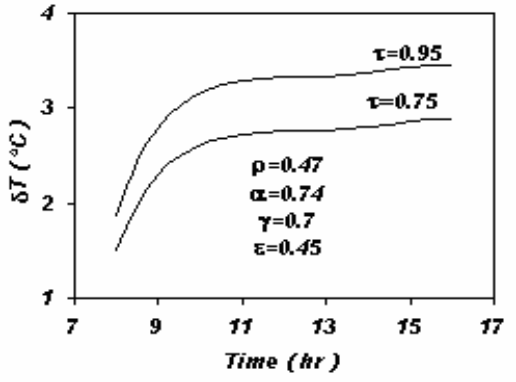


Fig. 12- Variation of oil temperature rise for various cover transmissivity

[Downloaded from necjournals.ir on 2026-11-18]

From the above analysis it is found that optical properties of the material used in the present collector are not appropriate and better quality material would improve thermal performances considerably. Based on this result, the optical properties is replaced by more practical values as presented in Table 2 and simulation is carried out for the same day and results are illustrated in Figs. 13-15. In Fig. 13 variation of oil and glass temperature during the day is shown. It is clear that oil outlet temperature exceeds 250 ^{o}C at 9 AM, which is much higher than those in Fig. 5. Corresponding optical and thermal efficiency is presented in Fig. 14. It can be observed that collector performances improved considerably. Figure 15 shows variation of solar irradiance and oil temperature rise. Comparing with Fig. 5, it is seen that temperature rise is improved similarly. More details about collector fields simulation is mentioned in [14].

Table 2. Optimized optical properties of the receiver and mirror

Reflectivity of mirror	0.94
Transmissivity of cover	0.965
Absorptivity of receiver	0.96
Emissivity of receiver	0.2
Intercept factor	0.95

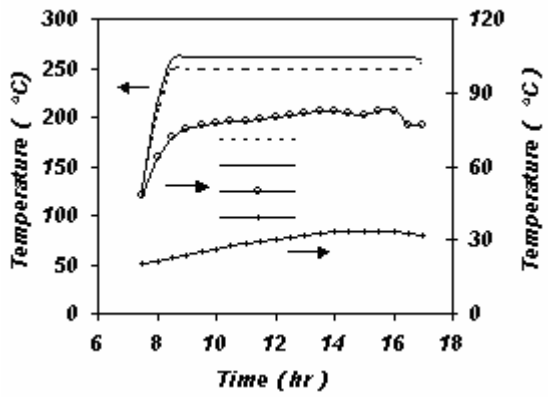


Fig. 13-Diurinal temperature for optimized optical properties

[Downloaded from necjournals.ir on 2026-11-18]

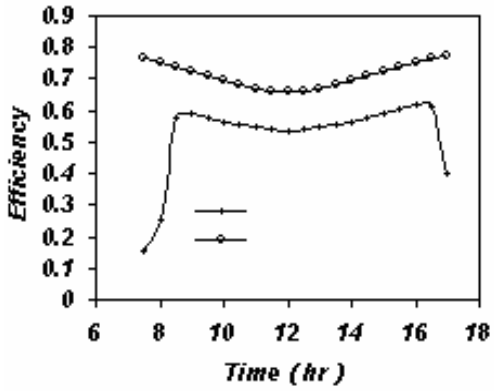


Fig. 14-Optimized thermal performances of the collector

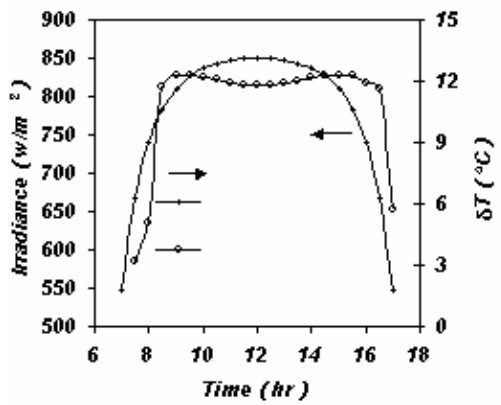


Fig. 15- Optimized variation of oil temperature rise in a single collector

Consideration the appropriate optical properties, a computer program is written to solve Eqs.(1-10) with FORTRAN language. To simulate the performance of the plant, three cities with high solar radiation potential, mainly in the central and southern part of Iran, are selected as shown in Table 3.

Table 3- The cities considered for simulation

City	Latitude	July			January		
		T_{max}	T_{min}	C_f	T_{max}	T_{min}	C_f
Shiraz	29°33′	37.3	19.6	0.191	12	-0.4	0.342
Yazd	31°34′	39.2	23.9	0.241	11.9	-0.9	0.419
Lar	27°40′	42.9	25.7	0.145	16.3	6	0.292

[Downloaded from necjournals.ir on 2026-11-18]

The outputs of program for each interval are oil temperature and flow rate from heat exchangers, collector heat absorption and efficiency, heat transfer to heat exchangers and heat transfer to the ambient. Results for twelve month of operation for Shiraz, Yazd and Lar is presented in Table 4,5,6.

Table 4- Annual operation and performances of the 250 KW solar plant in Shiraz

Month	Day	Sunrise	Sunset	Start Tracking	Start Steam Generation	Finish Steam Gen.	Finish Tracking	Qcol/QI	Qexch/QI	I/QI	Collector Eff. %	Cycle Eff. %
JAN	17	6:50	17:10	7:45	14:35	15:35	15:50	0.120	0.054	0.600	20.0	8.9
FEB	47	6:30	17:30	7:25	10:30	16:15	16:30	0.264	0.200	0.735	35.1	26.4
MAR	75	6:05	17:55	7:05	9:15	16:30	16:50	0.382	0.320	0.838	43.3	37.8
APR	105	5:39	18:21	6:40	8:35	17:05	17:25	0.508	0.426	0.878	49.0	48.0
MAY	135	5:16	18:44	6:15	7:45	17:40	17:55	0.623	0.586	1.140	54.4	51.2
JUN	162	5:04	18:56	6:05	7:25	17:50	18:05	0.704	0.657	1.260	55.0	52.1
JUL	198	5:09	18:51	6:10	7:35	17:45	18:00	0.656	0.620	1.180	55.0	52.1
AUG	228	5:29	18:31	6:30	7:45	17:30	18:50	0.641	0.603	1.180	54.2	51.0
SEP	258	5:55	18:05	6:55	8:10	17:00	17:20	0.590	0.549	1.170	50.0	47.0
OCT	288	6:21	17:39	7:20	8:55	16:35	16:50	0.428	0.367	1.010	42.3	36.3
NOV	318	6:44	17:16	7:40	12:20	16:00	16:15	0.225	0.120	0.735	30.5	16.2
DEC	344	6:55	17:05	7:50	14:10	14:50	15:10	0.140	0.033	0.604	23.0	5.6

Table 5- Annual operation and performances of the 250 KW solar plant in Yazd

Month	Day	Sunrise	Sunset	Start Tracking	Start Steam Generation	Finish Steam Gen.	Finish Tracking	Qcol/QI	Qexch/QI	I/QI	Collector Eff. %	Cycle Eff. %
JAN	17	6:50	17:10	8:00	14:45	15:20	16:00	0.112	0.049	0.567	18.3	8.4
FEB	47	6:30	17:30	7:30	13:20	16:05	16:20	0.244	0.185	0.667	32.6	24.9
MAR	75	6:05	17:55	7:05	9:55	16:40	17:00	0.357	0.292	0.778	39.5	35.8
APR	105	5:39	18:21	6:35	9:00	17:10	17:30	0.459	0.389	0.830	45.6	45.9
MAY	135	5:16	18:44	6:15	8:05	17:35	17:50	0.565	0.528	1.073	51.9	49.1
JUN	162	5:04	18:56	6:00	7:40	17:50	18:05	0.654	0.617	1.168	50.3	48.2
JUL	198	5:09	18:51	6:05	7:40	17:45	18:00	0.596	0.586	1.098	52.8	49.7
AUG	228	5:29	18:31	6:25	7:45	17:35	17:55	0.596	0.565	1.109	50.5	47.5
SEP	258	5:55	18:05	6:55	8:15	17:00	17:20	0.546	0.509	1.104	45.7	44.1
OCT	288	6:21	17:39	7:20	9:15	16:30	16:50	0.401	0.344	0.915	39.9	34.0
NOV	318	6:44	17:16	7:45	12:55	15:50	16:00	0.203	0.113	0.684	28.7	15.4
DEC	344	6:55	17:05	8:00	0:00	0:00	15:25	0.127	0.000	0.549	12.8	4.3

[Downloaded from necjournals.ir on 2026-11-18]

Table 6- Annual operation and performances of the 250 KW solar plant in Lar

Month	Day	Sunrise	Sunset	Start Tracking	Start Steam Generation	Finish Steam Gen.	Finish Tracking	Qcol/QI	Qexch/QI	I/QI	Collector Eff. %	Cycle Eff. %
JAN	17	6:46	17:14	7:40	10:45	16:20	16:45	0.134	0.060	0.688	22.0	9.6
FEB	47	6:27	17:33	7:25	9:15	16:35	16:55	0.303	0.227	0.825	37.4	28.7
MAR	75	6:05	17:55	7:00	8:30	17:00	17:20	0.435	0.361	0.949	46.8	40.6
APR	105	5:40	18:20	6:40	7:55	17:20	17:40	0.576	0.483	0.969	51.9	50.6
MAY	135	5:19	18:41	6:20	7:40	17:40	17:55	0.701	0.666	1.258	57.7	54.9
JUN	166	5:09	18:51	6:05	7:37	17:45	18:00	0.809	0.755	1.393	58.5	55.1
JUL	198	5:13	18:47	6:10	7:35	17:50	18:15	0.740	0.691	1.305	59.9	56.7
AUG	228	5:31	18:29	6:30	7:45	17:30	17:45	0.728	0.690	1.326	57.3	53.8
SEP	258	5:55	18:05	6:55	8:10	17:05	17:25	0.667	0.612	1.318	54.3	50.2
OCT	288	6:20	17:40	7:15	8:55	16:45	17:00	0.474	0.412	1.156	46.4	39.4
NOV	318	6:41	17:19	7:35	10:05	16:25	16:45	0.257	0.138	0.837	33.1	17.7
DEC	344	6:51	17:09	7:45	12:45	16:15	16:40	0.159	0.037	0.681	25.0	6.0

Table (4-6) show that tracking started early in the morning in summer, while for winter, tracking starts is late and steam generation period is short. Steam production reaches to zero in December in Yazd, using Daneshyar model. The difference between starts tracking and starts of steam generation is due to warning oil from around 160 ^{o}C to 240 ^{o}C. The heat absorbed by collectors after finishing steam generation, transferred to the storage.

Results for twelve months of operation for Shiraz, Yazd and Lar is also presented in Figures(16-18).In these figures the ratio of solar radiation absorbed, Qcol ,to the heat required by steam for 250 kw load, Ql , heat transfer in heat exchangers, ratio of incident radiation I/Ql, collector efficiency as well as overall oil cycle efficiency(heat transferred to steam/solar radiation to collector are shown.

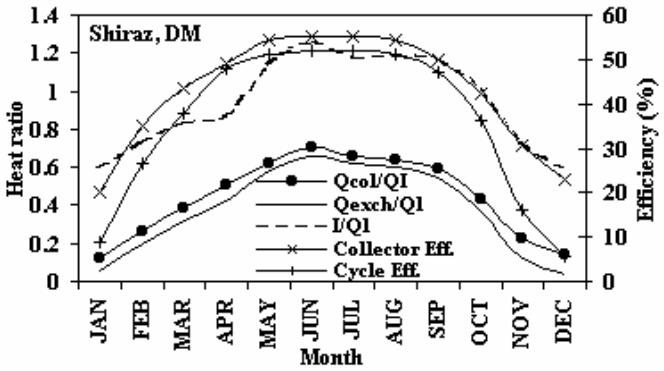


Fig. 16- The ratio heat absorbed by collectors, heat exchangers as well as efficiencies of collector and the oil cycle

[Downloaded from necjournals.ir on 2026-11-18]

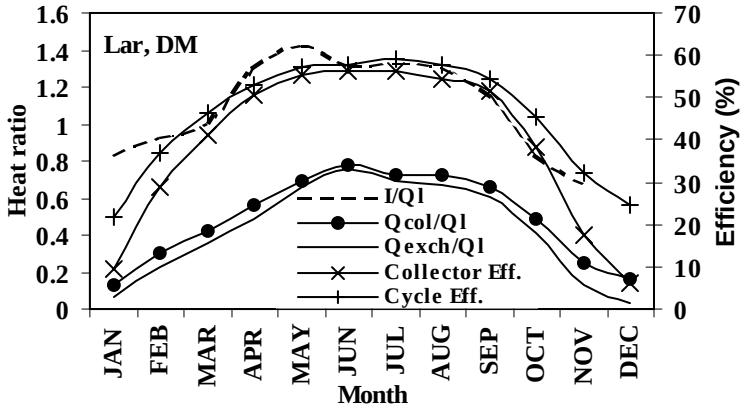


Fig.17 - The ratio heat absorbed by collectors, heat exchangers as well as efficiencies of collector and the oil cycle

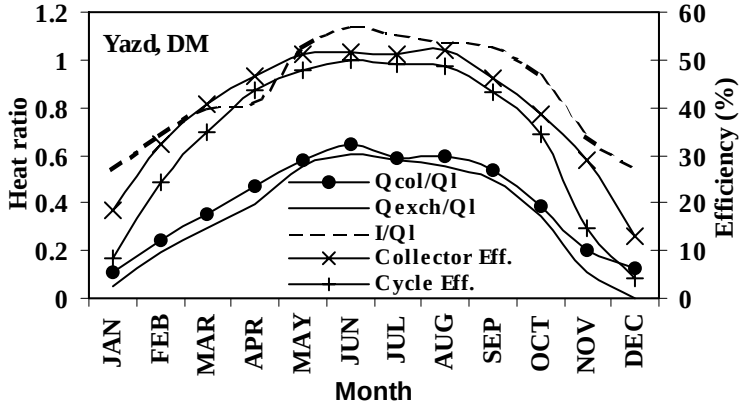


Fig. 18- The ratio heat absorbed by collectors, heat exchangers as well as efficiencies of collector and the oil cycle

The overall plant performance for each location is shown in Table 7.

Table 7- Plant performances for each location

City	$(Q_{exch}/Q_L)_{max}$	$(\eta_{cycle})_{max}$	Annual steam supplied
Shiraz	65.7%	52.1%	37.8%
Yazd	60%	53.1%	34.3%
Lar	71.6%	51.1%	40.2%

[Downloaded from necjournals.ir on 2026-11-18]

For all cities, maximum cycle efficiency is less than 60% in summer and maximum Qexch/Ql is less than 0.8.These values indicate that for the entire period of daytime of all days of a year, system is not able to generate steam for the rated power completely. Note, the system supply may exceed necessary supply for certain hours around noon. However, with clean sky solar radiation model results will be improved.

Conclusion

Based on the experimental measurement and mathematical simulation of the thermal performances of the solar collector and solar thermal power plant, it can be shown that:

1- Maximum performance of the present collector is much less than the design condition.
2- 2- Temperature rise in the receiver is more sensitive to the collector intercept factor as well as the mirror reflectivity.
3- For more appropriate optical properties of the collector, the field of collectors can easily produce hot oil with temperature around 275 ^{o}C after 8 AM in the summer.
4- With appropriate condition of the collectors' field, it would possible to produce steam and generate electricity in the turbine.
5- The best location for installing a solar plant is Lar, however, due to higher humidity in Lar and more dry conditions in Shiraz and Yazd, these cities are more appropriate locations.

For remote and south central part of Iran, solar power plant may contribute to supply more sustainable energy with less pollution generation and would be utilized with mach larger capacities within two decades.

Nomenclatures

A_c Area of the glass metal (m^2)
A_f Area of the oil section (m^2)
A_m Area of the pipe metal (m^2)
C_c Specific heat capacity of the glass metal (J/kg ^{o}C)
C_{fa} Cloud factor
C_f Specific heat capacity of oil (J/kg ^{o}C)
C_m Specific heat capacity of the pipe metal (J/kg ^{o}C)
d_{ci} Inner glass diameter (m)
d_{co} Outer glass diameter (m)
d_{ri} Inner pipe diameter (m)
d_{ro} Outer pipe diameter (m)
G Aperture of a collector mirror module (m)
H_{c-a} Heat transfer coefficient for glass to air (W/m^2 ^{o}C)
H_{c-r} Heat transfer coefficient for glass to metal (W/m^2 ^{o}C)
I_b Direct solar beam irradiance (W/m^2)
K_f Thermal conductivity of oil (W/m ^{o}C)
$K(\theta)$ Incidence-angle modifier
M_f Oil mass in pipe per unit length occupied(kg/m)
$\dot{m}_f$ Oil mass in pipe(kg/s)
P Perimeter of the tankn(m)
P_p Diameter of the pipes (m)
t Time (s)
T_a Ambient temperature (^{o}C)
T_c Glass metal temperature (^{o}C)
T_f Oil Temperature (^{o}C)
T_m Pipe metal temperature (^{o}C)
U Heat transfer coefficient from fluid to ambient(W/m^2 ^{o}C)

[Downloaded from necjournals.ir on 2026-11-18]

U_C Heat transfer coefficient for metal to oil ($W/m^2\,^oC$)
U_L Heat transfer coefficient for metal to air ($W/m^2\,^oC$)
V Oil velocity (m/s)
x Dimension of length (m)
α_c Absorption factor of glass tube
α Absorption factor of receiver
ε Remittance factor of receiver
γ Intercept factor
η_o Optical efficiency
θ Angle of incidence of the sun's rays on the collector aperture measured from the normal to the aperture
θ_z The angle of incidence of beam radiation on a horizontal surface
ρ Average specular reflectance of the reflective surface
ρ_c Density of the glass metal (kg/m^3)
ρ_f Density of the oil (kg/m^3)
ρ_m Density of the pipe metal (kg/m^3)
τ Transmittance factor of glass tube
$(\tau\alpha)_n$ Effective transmittance-absorptance factor at normal incidence

References

1- Broesamle, H., Mannstein,H., Schillings, C., Trieb,F., 2001, Assessment of Solar Electricity Potential in North Africa Based on Satellite Data and A Geographic Information System,Solar Energy,70:1-12

2- Cohen, G. E., D. W. Kearney and J. K. Gregory, 1999, Final Report on the Operation and Maintenance Improvement Program for Concentrating Solar Power Plants, SAND 99-1290.

3- Yaghoubi, M., A. Sabzevari, 1996, Further Data on Solar Radiation in Shiraz, Iran, Renewable Energy, 7(4): 333-339.

4- Yaghoubi, M., F. Doroodgar, 1996, Design of Parabolic Trough Collector for 250 KW Solar Power Plant, Journal of Iranian Energy 8(1): 54-62.

5- Meaburn, A., F. M. Huge, 1993, Resonance Characteristic of Distributed Solar Collector Field, Solar Energy, 51: 215-221.

6- Noory, P.,Yaghoubi, M 2000, Transient Analysis of the Thermal Performance of 250 KW Solar Power Plant, Iranian Journal of Energy,4(8):25-39.

7- Mehryar, R., 1997, Thermal Design of 250 KW Solar Power Plant to Generate Electricity in Iran, M.S. Thesis, Engineering School, Shiraz University.

8- Daneshyar, M., 1978, Solar Radiation Statistics for Iran, Solar Energy, 21: 345-350.

9- Guven, H. M., R. B. Bannerot, 1986, Determination of Error Tolerances for Optical Design of Parabolic Troughs for Developing Countries, Solar Energy, 36(6): 535-550.

10- Kenary, Gh., M. Yaghoubi and F. Doroodgar, 2000, Thermal Analysis of A Parabolic Trough Collector of 250 KW Power Plant, Proceedings of 4th International Chemical Engineering Conference, Shiraz, Iran, 9: 205-212.

11- Rabl, A., H. W. Gaul, 1982, Optimization of Parabolic Trough Solar Collectors, Solar Energy, 29:407-413.

12- ASTM, 1991, Standard Test Method for Determining Thermal Performance of Tracking Concentrating Solar Collectors, E905-87.

13- Mehryar, R., M. A. Yaghoubi, 1998, Design of 250 KW Mehr-Niroo Solar Thermal Plant, Proceedings of 2nd Int. Mechanical Engineering Conference, Shiraz, Iran, 503-510.

14- A.Kenary,M.Yaghoubi,F.Doroodgar,2001,Experimental and Numerical studies of A Solar Parabolic Trough Collector of 250 KW Pilot Solar Power Plant in Iran,Sharjeh Solar Energy Confrence,Book of Abstracts,Sharjeh,UAE,19-22 Februrary.

[Downloaded from necjournals.ir on 2026-11-18]